

Mechanical and Thermal Properties of Basalt Fibre Reinforced Polymer Rebars

Dr. V.Pavalan^a and Dr. R.Sivagamasundari^b

^aAssistant Professor, Department of Civil Engineering, Priyadarshini college of Engineering and Technology, Nellore, Andhra Pradesh

^bAssociate Professor, Department of Civil & Structural Engineering, Annamalai University, Tamil Nadu

Date of Submission: 10-11-2020

Date of Acceptance: 24-11-2020

ABSTRACT: The use of non-metallic fibre reinforced polymer (FRP) bars in concrete structures has widely increased in the construction sector due to their high mechanical performance. The Basalt FRP bars are a quite new FRP material for which the mechanical and thermal properties are yet to be completely addressed. This paper presents the results of mechanical and thermal properties of BFRP rebars which are essential to make use of BFRP bars as reinforcements in concrete structures. The BFRP rebars of diameters 8mm and 10mm were treated with surface treatment. The BFRP rebars were tested under tension, compression, pullout and thermal expansion coefficient tests. From the experimental test results, it was observed that the sand-coated BFRP bars show excellent qualities in all aspects.

Keywords: BFRP bars, Mechanical and thermal characteristics

I. INTRODUCTION

Steel rebars have been conventionally used as internal reinforcement for concrete structures all over the world. However, the researchers are not recommending the use of steel bars in marine and coastal areas. Many of structures like dry-docks, watertanks, box-culverts, floating piers reinforced with conventional steel bars can be corroded easily due to increase in age, de-icing salts and adverse environments. In several countries, the highway bridges are not safe due to deterioration caused by corrosion of steel reinforcements. To overcome these corrosion problems, researchers spotted a new non-metallic fibre reinforced polymer (FRP) material and it has been introduced as internal and external reinforcements for concrete structures. The use of fibre reinforced polymer reinforcements in concrete structures have been increased in the construction industry due to its excellent corrosion resistance, high tensile strength and lightweight characteristics. However, the modulus of elasticity of FRP bars is

relatively low compared to conventional steel bars. In recent years, carbon and glass fibre reinforced polymer materials have been widely used especially in marine fields. Basalt fibre reinforced polymer is a new type of FRP material in which mechanical properties are not yet fully described. The toughening mechanism between newly introduced FRP bars and concrete is the most critical aspect which affects the structural behaviour of the concrete structures. It is, therefore, necessary to investigate the bond behaviour of basalt fibre reinforced polymer bars.

Several experimental investigations on mechanical and thermal characteristics of basalt fibre reinforced polymer bars were reported (Ovitigala et al. 2009, Elgabbas et al. 2015, Refai et al. 2015, Ayadin 2018). Baena et al. (2009) investigated 88 concrete pull-out test specimens in accordance to ACI 440.3R (2004) and CSA (2002) standards. The influence of the reinforcement bar surface treatments, diameter of rebars and concrete strength on the bond-slip curves were studied for GFRP, CFRP and steel reinforcement. They stated that the strength of the concrete affects the mode of bond failure of the embedded steel rebar during the pull-out test. It was observed that, for concrete with compressive strength approximately greater than 4.35 ksi (30 MPa), the bond strength of FRP rebars does not depend greatly on the value of concrete strength, but rather on the reinforcement bar's properties since the bond failure occurs at the surface of the FRP reinforcement bars. Ovitigala (2012) sought to determine the mechanical properties of BFRP bars by testing five specimens of each of the five different bar sizes: 6, 10, 13, 16 and 25 mm. The tensile strength slightly decreased as the bar diameter increased, with values of 160.2 ksi (110.4 MPa), 162.6 ksi (1121.0 MPa) and 156.9 ksi (1081.7 MPa) for the 6 mm, 10 mm, and 13 mm bars, respectively. All rebar diameters exhibited a brittle failure by rupture of the fibers. Similarly, the modulus of elasticity of each bar size was also

determined and found to decrease with the increase of the rebar diameter, except for the 6 mm diameter rebar. The minimum value of 7260 ksi (50.0 GPa) was obtained from the 25 mm bars, while the 8 mm bars had the greatest modulus of 8022 ksi (55.3 GPa). As expected, the linear stress-strain curve continued until failure for all specimens. The ultimate strain at failure was as high as 20588 $\mu\epsilon$ for the 13 mm bars and 21171 $\mu\epsilon$ for the 6 mm bars. Elgabbaset al.(2015) concluded that the transverse coefficient of thermal expansion of BFRP specimens ranging from $18.4 \times 10^{-6}/^{\circ}\text{C}$ to $26.8 \times 10^{-6}/^{\circ}\text{C}$, which is less than $40 \times 10^{-6}/^{\circ}\text{C}$ as stated by Canadian standards association(CSA). Ayadin (2018) examined the thermal expansion coefficient of Glass FRP, Carbon FRP, Aramid FRP and Basalt FRP bars and concrete. The longitudinal coefficients of thermal expansion values of GFRP, CFRP, AFRP, and BFRP rebars were $4.43 \times 10^{-6}/^{\circ}\text{C}$, $1.05 \times 10^{-6}/^{\circ}\text{C}$, $-5.18 \times 10^{-6}/^{\circ}\text{C}$ and $1.92 \times 10^{-6}/^{\circ}\text{C}$, respectively. The transverse coefficients of thermal expansion values of FRP bars were $22.5 \times 10^{-6}/^{\circ}\text{C}$, $93 \times 10^{-6}/^{\circ}\text{C}$, $51 \times 10^{-6}/^{\circ}\text{C}$ and $17.1 \times 10^{-6}/^{\circ}\text{C}$, respectively. The longitudinal coefficients of thermal expansion of concrete were $6-8 \times 10^{-6}/^{\circ}\text{C}$ in different strengths. GFRP bar has been identified as the most stable material in its thermal behaviour whereas AFRP bar as the most unstable one. This paper presents the results of mechanical and thermal properties of surface coated BFRP rebar under tensile, compression, pull-out and thermal expansion coefficient tests.

II. EXPERIMENTAL PROGRAM

2.1. Materials

The sand coated BFRP bars of 8mm and 10mm- diameters were purchased from Arrow technical textile private limited, Mumbai, India and manufactured using pultrusion process. The bars were applied with standard epoxy resin and braided with nylon wire and then finally the quartz sand was coated on the bars as shown in Fig 1.



Fig.1 BFRP bars of different diameters

2.2 Mechanical Characteristics

2.2.1 Tensile test

The BFRP rebar specimens for tensile test were prepared according to the provisions of

ASTM D7205/D7205M-06(2006). The total length and the gauge length of BFRP rebar was 1000mm and 400mm, respectively. To prevent the failure end of clamped zone of BFRP rebar, the steel tube plugs and PVC caps were prepared with a hole of slightly larger than the diameter of the rebar. The steel tubes and PVC caps were fixed at the ends of rebar as shown in Fig. 2. A mixture of epoxy resin and hardener was used to fix the BFRP rebars with the steel tube at the ends. The first anchor was flipped after 24 hours to cast another anchor. The prepared tensile test specimens were cured for 28 days.

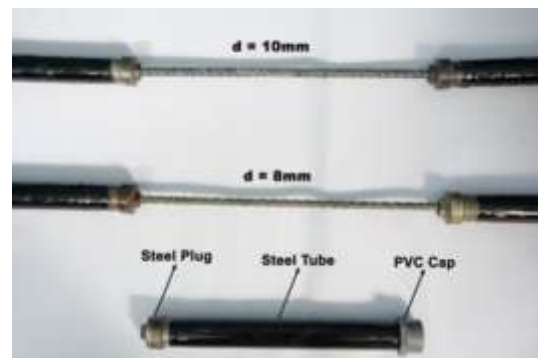


Fig. 2 Details of tensile specimen

The tensile test was performed by gripping the steel tube into the wedges of MTS testing machine with a capacity of 1000kN (Fig.3). The load was applied at a rate of 250MPa/min. An extensometer was attached at the mid-section of the BFRP rebar to measure the strain of the specimen with gauge length of 50mm. The applied load and BFRP bar extension was electronically recorded by a computerized data acquisition system. The ultimate tensile strength and modulus of elasticity were calculated by using following equations (1) and (2) respectively.

$$F_{tu} = P_{max} / A \quad (1)$$

$$E = (P_1 - P_2) / (\epsilon_1 - \epsilon_2) A \quad (2)$$

Where F_{tu} is ultimate tensile strength (MPa), P_{max} is the maximum force prior to failure (N), A is the cross-sectional area of the rebar (mm^2). E – modulus of elasticity (MPa); P_1 - 50% of maximum load (N); P_2 - 20% of maximum load (N) and ϵ_1 the strain corresponding to 50% of the maximum load; ϵ_2 the strain corresponding to 20% of the maximum load.



Fig.3. Tensile test setup

2.2.2 Compression Test

The compressive strength of rebar was carried out in accordance to ASTM D695-15 standards. The length of the test specimen was twice the diameter of the BFRPrebar. The specimen was placed axially between the platens of the compression testing machine. The load was applied at the rate of 1.0 to 1.3mm per minute and the failure load was noted using the computerized data acquisition system. Fig.4 shows the typical setup for compression test. The compressive strength of the BFRP bar was calculated as P_{max}/A , where P_{max} is the maximum applied force (N), A is the cross-sectional area of the bar (mm^2).



Fig.4. Compression test setup

2.2.3 Pull-out test

The pull-out specimens consisted of concrete cube of 200mm x 200mm x 200mm, with a 1200mm long BFRP bar embedded vertically along the axis of the specimen. The embedded length of the BFRP bar was five times the diameter of the BFRP rebar. The embedded bar was inserted within polyvinyl chloride (PVC) pipe to prevent bonding at top of concrete cube, and to avoid splitting of concrete during the pull-out test. Steel tubes were used as anchors at the loaded end of the BFRP bars and were cast with epoxy resin and hardener. All the pull-out specimens were cast in accordance with C192/C192M. The BFRP rebar

was held in position prior to pouring the concrete grade of MPa. The prepared pull-out specimens were cured in water for 28 days.

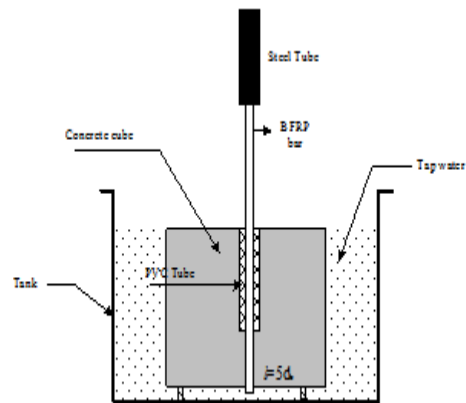


Fig.5 Geometry of the pullout specimens

The average bond stress can be calculated as the obtained maximum pull out force divided the surface area of the bar bonded to the concrete cube.

$$\tau = \frac{F}{C_b l} \quad (3)$$

Where, τ is the average bond stress (MPa), F is the tensile force (N), C_b is the equivalent circumference of BFRP bar, calculated as $3.1416d_b$ and l is the bonded length (mm). The slip of the BFRP bars in concrete can be achieved by,

$$s = s_L - s_F \quad (4)$$

Where, s is the slip of the BFRP bars (mm); s_L is the loaded end slip of the BFRP bar (mm); s_F is the free end slip of the BFRP bars (mm).

The bond strength of the BFRP rebar was evaluated by testing of eight specimens in accordance with ASTM D7913/D7913M-14. The steel tube anchorage at end of BFRP rebar was used to protect from crushing of the BFRP bar. This steel tube was clamped using the conventional wedge of frictional grips at lower jaw of Universal Testing Machine. The pull-out test was performed by pulling the steel tube at a load of 20kNmm until failure. Prior to the application of load, one linear variable differential transformer (LVDT) was attached to the top of extended free end of the BFRP bar to measure the vertical displacement using computer-controlled data acquisition system. Fig. 6 should the test set-up of pull-out test.

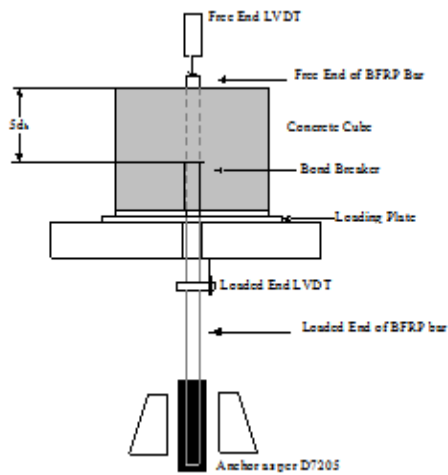


Fig.6 Pull-out test setup

2.3 Thermal Characteristics

The length and diameter of BFRP rebars used for Thermal expansion test was 30mm and 8mm, respectively. The thermal expansion test was performed using pushrod dilatometer at high temperature laboratory as shown in Fig.7. This pushrod dilatometer consists of furnace, inductive transducer, temperature sensor, and specimen holder. The initial length of the specimen was noted at room temperature. Subsequently, the specimen was placed into a holder of the pushrod dilatometer. A spring-loaded pushrod was positioned against the specimen. The opposite end of the push rod was connected to a displacement sensor. The specimen and holder were enclosed within a furnace where the specimen was heated at a constant rate 2^oC/min up to a temperature of 350^oC. During the experiment, the linear thermal expansion of the specimen was measured at every 50^oC using a highly accurate displacement sensing system. The thermal expansion coefficient (α) can be determined by the following equation.

$$\alpha = \frac{1}{L_o} \frac{\Delta L}{\Delta T}$$

(5)

Where, L_o is the initial length of the specimen at room temperature (^oC); ΔL is the change in length of the specimen(mm) and ΔT is the temperature difference between any two temperatures T_o and T_1 (^oC).



Fig.7 Opened pushrod dilatometer

III. RESULTS AND DISCUSSION

3.1. Mechanical characteristics

3.1.1 Tensile test

The ultimate tensile strength and modulus of elasticity of BFRP and conventional steel bars are tabulated in Table1. All the BFRP specimens were failed in the free length through the rupture of fibres as shown in Fig.8. According to the test results, the ultimate tensile strength of the BFRP bars was 3 times higher than that of conventional steel bars, and the modulus of elasticity was about 1/4 of the conventional steel bars. After tensile testing, the steel tube anchors of the specimens were cut through saw blade at both ends to notice the condition of the BFRP bars(Fig.9).

Table 1 Tensile test results of Sand-coated BFRP bars

Specimen	Peak Tensile load (kN)	Peak Tensile Extension (mm)	Ultimate Tensile Strength (MPa)	Elastic Modulus (GPa)
BF-8-1	70.2	20.1	1396.5	49.5
BF-8-2	68.3	19.4	1358.7	48
BF-8-3	69.7	19.8	1386.5	49.4
BF-8-4	69.5	19.7	1382.5	48.7
BF-8-5	69.6	19.5	1364.6	48.6
BF-10-1	114.8	38.9	1461.6	50.3
BF-10-2	116.2	40.3	1479.5	50
BF-10-3	115.7	39.3	1473.1	50.6

BF-10-4	117.1	40.4	1490.8	50.9
BF-10-5	115.2	39.3	1470.7	50
STEEL	46.5	37.6	593.3	200



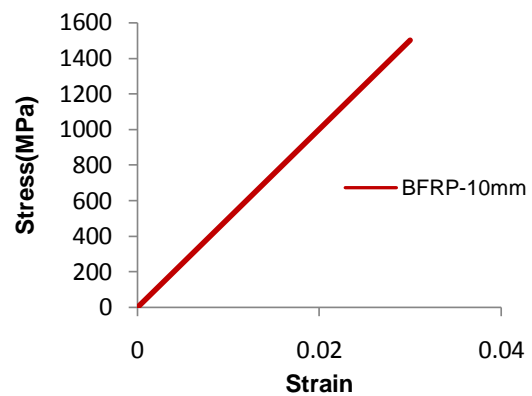
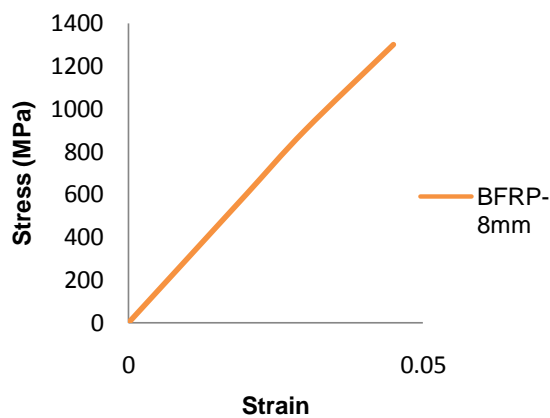
Fig. 8BFRP Rupture Failure of tensile specimens



Fig.9 BFRP bar ends in the steel tube anchors after tensile test

The stress-strain curve of Steel and BFRP rebar is shown in Fig. 10. From the figure, it can be seen that the stress-strain curves of the BFRP bar was linear and it does not have any yield point up to the failure. The stress-strain curves of the

BFRP bars are almost similar with different diameters. The stress-strain response of steel bars beyond the elastic portion, yielding occurs at the beginning of plastic deformation.



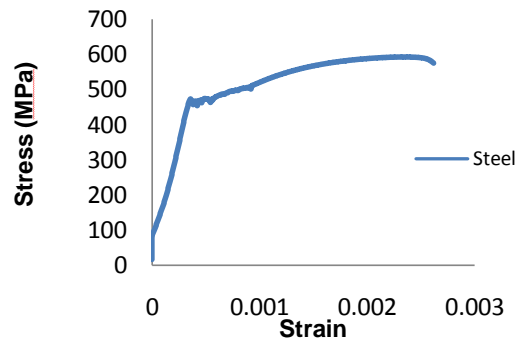


Fig.10 Stress –Strain curve of Steel and BFRP bars of different diameters

3.1.2 Compression Test

The peak compressive stress of tested BFRP bars was given in Table 2. Typical failure mode of the BFRP bars under compression as shown in Fig.11. It is observed that the failure of BFRP bars occurred due to crushing of longitudinal

fibres. According to the compression test results, the ultimate compressive strength is three times lesser than the ultimate tensile strength of the BFRP bars. The ultimate compressive strength of the BFRP bars varies a smaller amount with the increase of diameter.

Table 2 Compression test Results of sand-coated BFRP bars

SpecimenID	Peak Compressive Load (kN)	Peak Compressive Deformation (mm)	Compressive strength (MPa)
BFRP8	30.5	0.40	470.2
BFRP10	37.1	0.45	480.6



Fig.11. Typical failure mode

3.1.3 Pull-out test

The bond strength of sand-coated BFRP rebars of 10mm diameter is given in Table 3. All BFRP specimens were failed in typical pull-out failure mode. No visual cracks were noticed on the BFRP embedded concrete cubes. After testing, the

pull-out specimens were split to visually assess the conditions of the bar and concrete surface along the embedded length. It was observed that the rebar and concrete surface was not damaged at loaded end. Close to the free end, the surface layer of the bar was partly peeled off.

Table 3 Pull-out test results of Sand-coated BFRP bars

Specimen	Compressive Strength (MPa)	Pullout Load (kN)	Bond Strength (MPa)	Failure Mode
B10-L60-1	48.5	33.06	17.53	Pullout failure
B10-L60-2	48.5	35.62	18.89	Pullout failure
B10-L60-3	48.5	31.68	16.81	Pullout failure
B10-L60-4	48.5	29.31	15.54	Pullout failure
B10-L60-5	48.5	33.70	17.87	Pullout failure

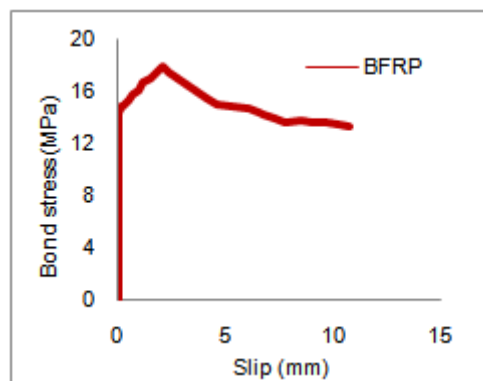


Fig.12. Bond stress-slip response of BFRP specimens

Fig. 12 shows the bond stress – slip response of BFRP rebar. The rebar bond slip at 50% of ultimate bond stress was 78 % lesser the ultimate bond slip value. The rebar slip was not obtained in all the specimens at free ends (unloaded ends) until the specimen reached to ultimate load whereas the loaded end slip was obtained in all the specimens at all stages of loading. The maximum bond stress and corresponding slip was noted in all the specimens at free ends, these slips are very smaller (0.09mm). At loaded ends, the slips of 3.65mm were reached at maximum bond stress. The bar slip of free ends were notably smaller than the loaded ends at all stages of loading. However, the high initial stiffness was observed between BFRP bar and concrete at loaded and unloaded ends.

3.2 Thermal Characteristics

The thermal expansion coefficient values of sand-coated BFRP bars of 8mm-diameter are shown in Table 4. From the experimental test results, it was observed that the thermal expansion coefficient of sand-coated BFRP bars was about 2.74×10^{-6} at 100°C and increased up to 4.65×10^{-6} at 300°C . At 350°C , the amount of expansion decreased thereby decreasing its CTE due to the oxidation of the resin and thus possible deterioration of the interfaces initiated between fibre and resin matrix. When the sand-coated BFRP bars were heated to the temperature above 300°C , a smoke was raised from the pushrod dilatometer.

Table 4 CTE test results of Sand coated BFRP bars

Specimen ID	Temperature ($^{\circ}\text{C}$)	Thermal Expansion (mm)	Thermal Expansion Coefficient ($/^{\circ}\text{C}$)
BFRP8-1	100	0.004	2.74×10^{-6}
BFRP8-2	150	0.008	3.09×10^{-6}
BFRP8-3	200	0.016	3.94×10^{-6}
BFRP8-4	250	0.024	4.45×10^{-6}
BFRP8-5	300	0.031	4.65×10^{-6}
BFRP8-6	350	0.027	3.66×10^{-6}

IV. CONCLUSION

The mechanical and thermal characteristics results of sand-coated BFRP bars were tested and presented. The ultimate tensile strength of the tested BFRP bars was varied between 1378 and 1475 MPa, however the elastic modulus was varied between 48 to 50 GPa. BFRP bars achieved a compressive strength value which is half of its tensile strength value. The ultimate compressive strength of the BFRP bars varied slightly with the increase of diameter. The bond stress-slip response has been mainly controlled by the surface treatment of the BFRP bars. The thermal expansion coefficient of sand-coated BFRP bars was about 2.74×10^{-6} at 100°C and increased up to 4.65×10^{-6} at 300°C . At high temperature (350°C), the degradation of the polymer matrix was observed and they led to a decrease of the CTET. Thus, the sand-coated BFRP bars have proven its distinguished qualities throughout the present study.

REFERENCES

- [1]. Baena, M., Torres, L. I., Turon, A., Barris, C. (2009). "Experimental study of bond behaviour between concrete and FRP bars using a pull-out test", *Composites, Part B Engineering*, 40 (8), 784–97.
- [2]. Ovitigala, T. (2012). "Structural behaviour of concrete beams reinforced with Basalt Fibre Reinforced Polymer (BFRP) bars", PhD Thesis, University of Illinois, Chicago.
- [3]. Elgabbas, F., Ahmed, E.A., Benmokrane, B. (2015). "Physical and mechanical characteristics of new basalt-FRP bars for reinforced concrete structures", *Construction and building materials*, 95(1), 623-635.
- [4]. Refai, A. El., P.E., Ammar, M.A., Masmoudi, R. (2015). "Bond performance of basalt fiber-reinforced polymer bars to concrete", *Journal of composite construction*, 11, 040140501-12.
- [5]. Ayadin, F. (2018). "Experimental investigation of thermal expansion and concrete strength effects on FRP bars behavior embedded in concrete," *Construction and Building Materials*, 163(5), 1-8.
- [6]. ASTM: D7205/7205M (2006). "Standard Test Method for Tensile Properties of Fiber Reinforced Polymer Matrix Composite Bars", ASTM International, USA.
- [7]. ASTM: E228 (2011). "Standard test method for Linear thermal expansion of solid materials with a push-rod dilatometer", ASTM International, USA.
- [8]. ASTM: D7913/D7913M (2014). "Standard Test Method for bond strength of fiber-reinforced polymer matrix composite bars to concrete by pull out testing", ASTM International, USA.
- [9]. ASTM: D695 (2015). "Standard Test Method for compressive properties of rigid plastics", ASTM International, USA.
- [10]. ASTM C192/C192M (2019). "Standard Practice for Making and Curing Concrete Test Specimens in the Laboratory", ASTM International, USA.